


Spring 5-10-2014

Mechanism of Insulin Aggregation: Applied to Alzheimer's Disease

Milos Atz

University of Connecticut, milos.ivo.atz@gmail.com

Follow this and additional works at: https://opencommons.uconn.edu/srhonors_theses

 Part of the [Biochemical and Biomolecular Engineering Commons](#), and the [Polymer Science Commons](#)

Recommended Citation

Atz, Milos, "Mechanism of Insulin Aggregation: Applied to Alzheimer's Disease" (2014). *Honors Scholar Theses*. 378.
https://opencommons.uconn.edu/srhonors_theses/378

University of Connecticut Honors Program

Mechanism of insulin aggregation: Applied to Alzheimer's disease

Honors Scholar Thesis, Chemical Engineering

Miloš Atz¹

Ming Li², Georges Belfort^{3,4}, Mu-Ping Nieh^{1,2}

¹*Department of Chemical and Biomolecular Engineering, University of Connecticut, 191 Auditorium Rd Unit 322, Storrs, CT 06269*

²*Institute of Materials Science, University of Connecticut, 97 North Eagleville Rd, Storrs, CT 06269*

³*Howard P. Isermann Department of Chemical and Biological Engineering, Rensselaer Polytechnic Institute, Troy, NY 12180*

⁴*Center for Biotechnology and Interdisciplinary Studies, Rensselaer Polytechnic Institute, Troy, NY 12180*

Table of Contents

Table of Figures	1
Abstract	2
Introduction	3
Experimental Procedure	7
<i>Materials</i>	7
<i>Sample Preparation</i>	7
<i>Sample Heating</i>	8
<i>Dynamic Light Scattering</i>	9
<i>Data Analysis</i>	11
Results and Discussion	13
<i>Preliminary results</i>	13
<i>Study results</i>	15
Conclusions and Future Work	23
References	24

Table of Figures

<i>Figure 1: Proposed mechanism of insulin aggregation.</i>	5
<i>Figure 2: Scattering intensity at 90° of human insulin at 60°C as a function of annealing time...</i>	6
<i>Figure 3: Heat block map.</i>	8
<i>Figure 4: Example sample heating history.</i>	9
<i>Figure 5: Insulin scattering intensity measurements taken after 5, 10 minutes heating.</i>	13
<i>Figure 6: Insulin scattering intensity measurements taken after 15 minutes heating.</i>	14
<i>Figure 7: Insulin scattering intensity measurements taken after 20 minutes heating.</i>	15
<i>Figure 8: Autocorrelation functions at various times after removal from heat.</i>	17
<i>Figure 9: Hydrodynamic radii peak distributions and mean particle sizes.</i>	18
<i>Figure 10: Calculated hydrodynamic radius peak distribution widths after removal from heat.</i>	19
<i>Figure 11: Peak broadening versus time after removal from heat for all samples.....</i>	20
<i>Figure 12: Scattering intensity data versus time after removal from heat for samples heatedy..</i>	21
<i>Figure 13: Intensity increase from preheat baseline versus time after removal from heat.....</i>	22

Abstract

Alzheimer's disease, a debilitating neurodegenerative illness, is caused by the irreversible aggregation of beta-amyloid proteins in the brain. In Alzheimer's brains, the protein can become disfigured, causing it to aggregate into long, insoluble fibers that deposit on brain tissue.

Studying the aggregation mechanisms of amyloid proteins can lead to a deeper understanding of the progression of Alzheimer's disease and possibly point towards a potential cure or treatment for the disease. Heat induced aggregation of insulin provides a model system to study the aggregation of amyloidogenic proteins. This study investigates the early stages of heat induced insulin aggregation using dynamic light scattering in order to assess the aggregation mechanism and the potential for reversal by thermal quenching to room temperature. In order to accomplish this, samples of insulin solution were heated for specific incubation intervals and monitored using dynamic light scattering in the time after removal from heat to study the behavior of insulin after quenching to room temperature. Results indicate that large protein aggregates form after sufficient time at heat, but quenching to room temperature can cause them to dissociate. However, the initial stage in the aggregation mechanism is shown to be an irreversible transformation from monomer to dimer.

Introduction

Alzheimer's disease is an irreversible neurodegenerative disease that slowly attacks memory and degrades brain function⁽¹⁾. The disease affects primarily older patients and is the most common cause of dementia among older people⁽¹⁾. According to the Alzheimer's Association, one in eight older Americans – a population totaling 5.4 million - are living with Alzheimer's disease⁽²⁾. It is the sixth-leading cause of death in the United States⁽²⁾. Some medications can help lessen symptoms such as memory loss and confusion, but unlike the other top ten causes of death in the United States, there is currently no way to cure, prevent, or slow the progression of Alzheimer's disease⁽³⁾⁽⁴⁾. Thus, there is an urgent need to understand the cause of and find a cure for Alzheimer's disease.

The appearance of long, insoluble protein deposits on brain tissue is a common characteristic of many neurodegenerative diseases, including Alzheimer's disease⁽⁵⁾. The deposits, called plaques and tangles, are found between and around neurons in Alzheimer's disease patients' brains⁽²⁾. These buildups are made up of beta-amyloid proteins that are produced from amyloid precursor protein (APP) in the fatty membrane surrounding nerve cells⁽⁶⁾⁽⁷⁾. APP can be found in healthy brains as a precursor for other proteins that promote neuronal growth and survival. However, by an alternative pathway, APP forms beta-amyloid peptides that become disfigured, causing the formation of fibril aggregates with other beta-amyloid peptides. It is presumed that specific sizes of beta-amyloid aggregates in block cell communication and disrupt processes that normal cells need to survive⁽²⁾. It has been shown that mice injected with beta-amyloid fibril "building blocks" develop symptoms characteristic of Alzheimer's disease⁽⁸⁾. The continued growth of these smaller aggregates leads to the production of plaques on brain tissue⁽⁷⁾. In order to prevent or cure Alzheimer's disease, it is important to understand the aggregation mechanism and the potential for aggregation-reversal of the beta-amyloid peptide.

Historically, much work has been performed on the properties and aggregation of amyloid proteins, including the beta-amyloid peptide. It is currently believed that the aggregation of beta-amyloids is caused by a partial unfolding of the protein. The protein undergoes a coil-to- β -sheet transition and subsequently self-associates due in part to the exposure of hydrophobic regions within the tertiary structure. It is believed that the subsequently formed oligomers and protofibrils are the building blocks for mature, insoluble fibrils ⁽⁶⁾.

It has been found that amyloid proteins exhibit similar aggregation behaviors that can be caused by a number of factors such as pH and elevated solution temperature. These two in particular have been the classical methods of inducing amyloid aggregation ⁽⁹⁾. Human insulin, for example, is a classic amyloidogenic protein that aggregates at high temperature (> 60°C) in acidic solution (pH = 1.6). After sufficient exposure to high temperatures, insulin in acidic solution will form long, insoluble fibers. The absorbance intensity of aggregating insulin exhibits a sigmoidal curve, increasing as aggregation progresses. Initially, the intensity increase is slow, but this is followed by a rapid increase as the insulin aggregates into fibrils. After this rapid fibril formation, the growth saturates, and the rate of intensity increase becomes zero. Many studies have shown that protein fibers eventually form at the end of the annealing process ⁽⁹⁾. It is known that the formation of amyloid protein fibers is irreversible, although it is unclear at what point irreversibility is attained. Since insulin is relatively inexpensive, readily available, and exhibits a similar molecular and fibril structure to beta-amyloids, it is an ideal model system to study beta-amyloid aggregation ^{(10) (11) (12)}. By studying the amyloid aggregation in this model system we can gain a better understanding of the cause of – and a possible mechanism to inhibit or cure – the underlying causes of Alzheimer’s disease.

Insulin heat precipitation does not significantly alter the natural structure of the molecules, thus making it an ideal way to analyze the aggregation process. The aggregation itself

is a process understood to be comprised of three reactions. The first is nucleation, the slowest of the three, involving the simultaneous interaction of three to four insulin monomers. The second reaction is the growth of the nucleus into fibrils and the third is the formation of large precipitate groups. The large precipitate groups are generally irreversibly insoluble without major changes in solution characteristics⁽⁹⁾. A proposed mechanism of insulin fibrillation is diagrammed in Figure 1, though the actual mechanism is still under investigation⁽¹⁰⁾.

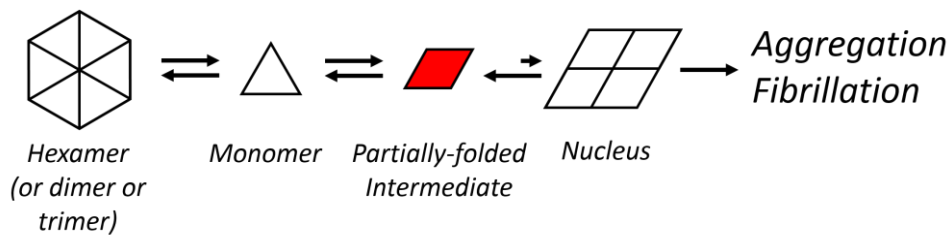


Figure 1: A proposed mechanism of insulin aggregation⁽¹⁰⁾.

Preliminary kinetic studies using dynamic light scattering (DLS) were performed on insulin in acidic solution (pH = 1.6) at 2 mg/ml. It is known that the scattering intensity is proportional to the size of the aggregates at a constant concentration. Figure 2 shows the scattering intensity variation (scattering angle = 90°) of insulin aggregation at 60°C as a function of annealing time. As previously mentioned the data follows a sigmoidal curve, though only the initial portion is shown. The early stage (< 140 min) of the aggregation indicated an incremental increase in scattering intensity. A sudden increase in scattering intensity was observed after approximately 150 minutes and beyond this point the average scattering intensity fluctuates drastically due to many intensity spikes recorded over the data collection time, indicative of the formation of large and non-uniform aggregates. These results point towards an early aggregation stage that takes place by a step-by-step process until a certain point is reached and the fibrillation becomes rapid.

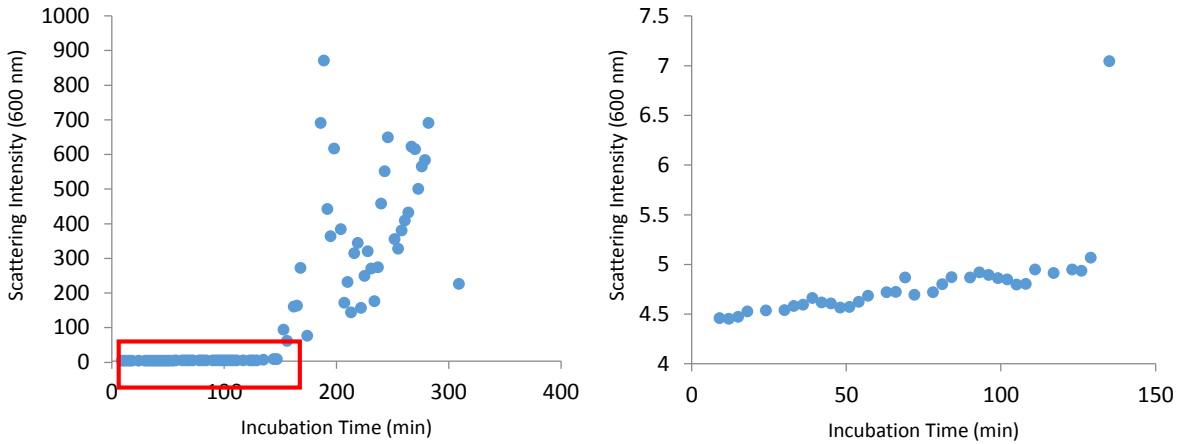


Figure 2: (a) The scattering intensity at 90° of human insulin at 60°C as a function of annealing time. For better resolution, the enlarged plot of the early stage aggregation of the insulin (in red box) is shown in (b).

Figure 2 makes apparent the initially-slow heat induced aggregation of insulin. This study assumes that irreversibility by thermal quenching – removal from heat to a room temperature environment – is attained very early in the aggregation process, before fibrils are formed and insulin aggregates become insoluble. Thus, the area of interest on the sigmoidal curve is early, before rapid aggregation begins. The earliest portion of this slow stage will be investigated to assess the potential reversibility of aggregation by thermal quenching. It is hypothesized that irreversibility is attained at heating times between 10 and 20 minutes. The goal of this study is to find that point of irreversibility and show that before that point is reached, reversal of insulin aggregation can be performed.

Experimental Procedure

Materials

Human insulin was provided by Professor Georges Belford and his group at Rensselaer Polytechnic Institute. All reagents and chemicals are analytical grade.

Sample Preparation

Solutions of human insulin in concentrations of 20 mg/ml are made by dissolving 40 mg insulin in 2 ml of a previously prepared “insulin solvent” of 100 mM NaCl and 25 mM HCl of pH 1.6. The solutions are titrated to basicity with 1M NaOH. Insulin is not soluble near its pI of 5.6 and comes out of solution. NaOH addition is stopped once the solution becomes sufficiently basic for the insulin to redissolve. The solutions are then back-titrated using the insulin solvent, again just past the point of insulin redissolution. After titration, two solutions (up until this point prepared in parallel) are combined, diluted to 8 mg/ml using the insulin solvent, and adjusted to a pH of 1.6 with 1M HCl using a Thermo brand pH meter. Dust and large particle contaminants are removed by filtering the solutions through 0.2 μm hydrophilic filters at multiple stages of the process, including before the sample pH cycle titrations and after the pH adjustment to 1.6. The samples are divided into light scattering cuvettes, with approximately 1 ml of insulin solution in each. The cuvettes are sealed and the samples are checked for uniformity of size (~ 2.2 nm hydrodynamic radius for monomeric insulin) using dynamic light scattering. The samples are stored in a refrigerator to suppress unwanted protein activity.

Sample Heating

Aggregation is induced by placing the glass cuvettes into a dry heat block, set on Low, Power Level 9 for a measured temperature of 65°C. The amount of time required for a 1 ml sample in a glass DLS cuvette to reach 65°C, the incubation temperature, is dependent on the sample position in the heat block. A temperature map of the heat block was created, shown in Figure 3. The well that was selected for use is marked by an asterisk. In this well, approximately seven minutes are required for the sample to reach the incubation temperature.

The samples are allowed this warm up time to reach 65°C and then further incubated for set intervals of time. An example heating schedule is shown in Figure 4, where the sample is warmed, incubated, and removed from heat. Immediately after removal from heat, the samples are measured by DLS. This entire process is performed on one sample at a time in order to ensure uniformity in heating and measurement.

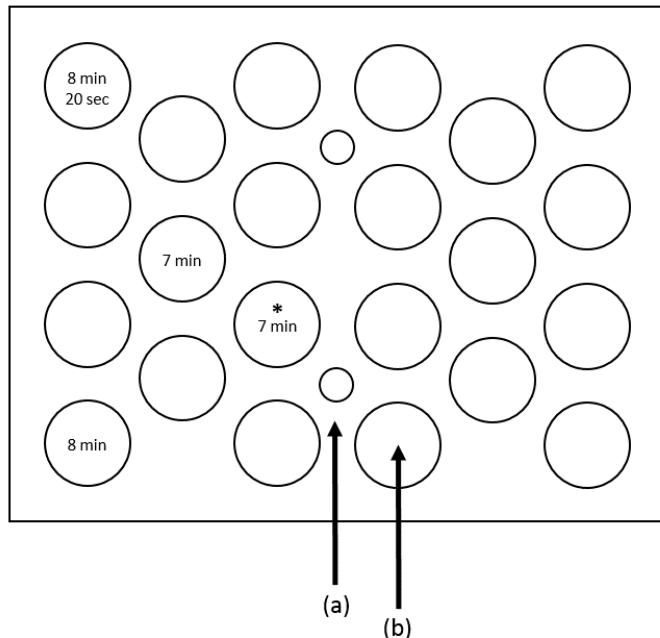


Figure 3: Heat block map. (a) Thermometer well. (b) Sample well. The well used for sample heating is denoted by an asterisk and was chosen based on the proximity to the thermometer and the minimal time taken to reach 65°C.

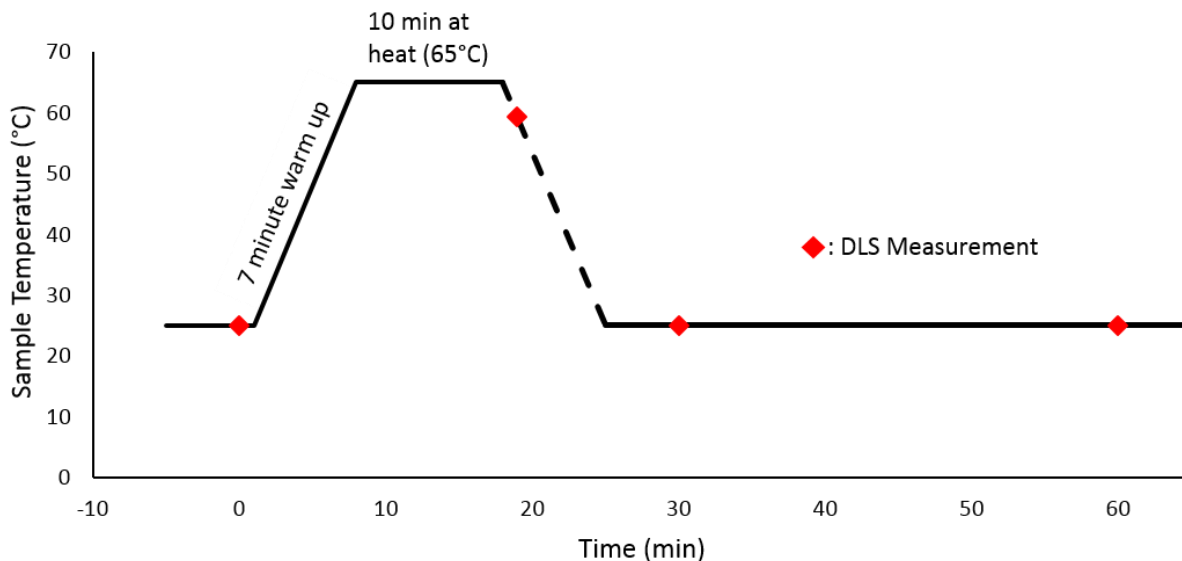


Figure 4: Example sample heating history. The red diamonds indicate DLS measurements (initial measurement not shown). The dotted black line represents unknown temperature decrease back to room temperature.

Dynamic Light Scattering

The quality of prepared insulin samples and the assessment of their aggregation is performed using dynamic light scattering (DLS). DLS is a powerful analytical method for determining the hydrodynamic radius of particles in solution. The instrument itself is an ALV Compact Goniometer System (CGS-3MD), consisting of a 22mW He-Ne laser that emits vertically polarized light at a wavelength of 632.8 nm and four avalanche photo diode (APD) detectors that collect the intensity of the scattered light⁽¹³⁾⁽¹⁴⁾. For this study, single detector mode was used with a scattering angle (θ) of 90°.

When the laser light hits particles in solution, it scatters in all directions due to Rayleigh scattering. Because the laser is monochromatic and coherent, the detector observes a time-dependent fluctuation in intensity due to the Brownian motion of the particles in solution. This variable intensity is collected by the detectors and an autocorrelation function is generated to relate the delay time, τ and scattering intensity, I . The autocorrelation function is generated by an ALV-7004 digital multiple tau real time correlator and expressed as Equation 1.

$$G(\tau) = \int_0^{\infty} I(t)I(t + \tau)dt \quad (\text{Equation 1})$$

In Equation 2, time delay, τ , refers to an arbitrary amount of time after the intensity measurement was taken (time = t). As τ grows larger, $G(\tau)$ exhibits an exponential decay as the correlation between the initial state and final state scattering intensities deteriorates. This relationship preserves the dynamic information of the particles in solution. Additionally, it has the ability to reflect system polydispersity, because populations of different sizes exhibit different decay times. Multiple decays can be shown within one autocorrelation function. Further experimental conditions are considered in a relationship expressing $G(\tau)$ in terms of the field autocorrelation function, $g(\tau)$, generated from the Siegert relation.

$$G(\tau) = 1 + \gamma g(\tau)^2 \quad (\text{Equation 2})$$

Here, γ is the instrumental coherence factor. The field autocorrelation function, $g(\tau)$, represents the time decay of the position autocorrelation function of the particles. For a polydisperse system, $g(\tau)$ can be expressed as follows.

$$g(\tau) = \sum_i A_i e^{-D_i q^2 \tau} \quad (\text{Equation 3})$$

$$\text{where: } q = \frac{4n\pi}{\lambda} \sin \frac{\theta}{2} \quad (\text{Equation 4})$$

In this expression, q is the scattering vector and A_i represents the light scattering amplitude of the particle i with diffusion coefficient D_i ⁽¹⁴⁾. For solutions made up of spherical, non-interacting particles undergoing Brownian motion, the Stokes-Einstein equation relates the particle radius, R_i , and the diffusion coefficient, D_i .

$$D_i = \frac{kT}{6\pi\eta_w R_i} \quad (\text{Equation 5})$$

Here, k , T , and η_w are the Boltzmann constant, absolute temperature, and the viscosity, respectively. In this case, the viscosity is that of water (the solvent). The geometry of aggregating insulin is not spherical, so R_i is replaced in Eq. 1 by R_{Hi} , an equivalent hydrodynamic radius.

Thus, the size of particles in solution is obtained. The ALV software analyzes the generated autocorrelation function using CONTIN procedure. The algorithm is ideal for polydisperse and multimodal systems – for instance, a solution of aggregating insulin with particle populations of different sizes ⁽¹⁵⁾⁽¹⁶⁾.

The insulin samples are analyzed with DLS before and after heating, allowing for detailed analysis of particles in the solution. Three to five measurements at room temperature lasting 60 seconds each are taken immediately after the samples are removed from heat. Identical sets of measurements are repeated again 30 and/or 60 minutes after removal from heat, once the samples have been allowed to rest at room temperature, and additionally 24+ hours after heating. The scattering intensity, autocorrelation function, and particle size distribution data are collected and analyzed over all measurement points in order to observe the insulin aggregation after removal from heat.

Data Analysis

The ALV700X software outputs data in multiple forms. Most of this data is interpretable as produced, but some, namely the size distribution data of the particles in solution, needs additional work in order to generate quantifiable figures. Custom MATLAB code was written in order to analyze this data. The code intakes Excel files filled with peak distribution data points. Iterating over data sets for all measured samples, it calculates peak width by identifying the maximum point on the distribution peak (which is equal to, by definition, 1) and then the derivative as it moves to the next point on left of the peak. It repeats this process until the derivative is null, at which point the program has reached the left boundary of the peak. This point is saved, the process is repeated to the right of the peak. The difference of the two saved

points is calculated as the peak width. The program records all data back into the Excel sheet from which it was originally read.

Results and Discussion

As described previously, ALV700X software produces data in the forms of the measured scattering intensity, the generated autocorrelation function, and the hydrodynamic radius distribution. A preliminary study, different from the one proposed in the *Sample Heating* section, was carried out before the development of the aforementioned procedure using identical insulin samples. The details and results of this study and the formal procedure are described below.

Preliminary results

Initial studies on solutions of insulin revealed the possibility of reversal by thermal quenching. Samples of insulin were heated for increments of 5 minutes, allowed to equilibrate to room temperature, and monitored with DLS. The most telling result of this preliminary study was the measured scattering intensity, which is proportional to the particle size when the concentration remains constant.

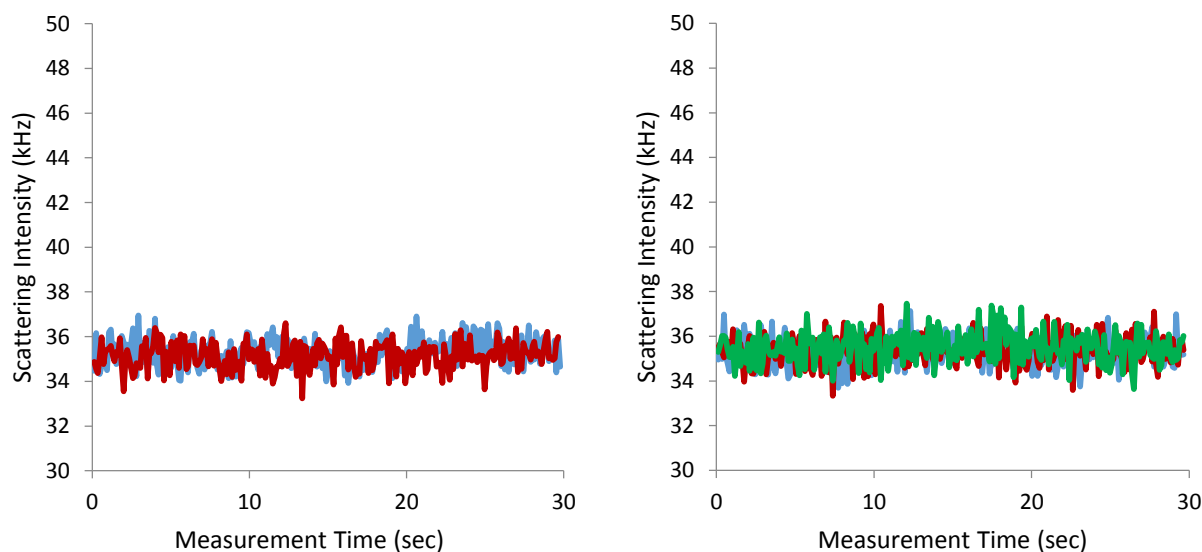


Figure 5: Insulin scattering intensity measurements taken after (a) one, and (b) two 5-minute heating periods (totaling 5 and 10 minutes at heat, respectively). The multiple lines represent repeated measurements.

After one 5-minute increment of heating and equilibration to room temperature, the average scattering intensity was equal to that of the initial measurement at 35 kHz. No intensity change was realized. After two 5-minute heating increments, totaling 10 minutes of heating, a slight increase in average scattering intensity was realized, but no substantial change was present. The results are visible in Figure 5, which shows the intensity measurements versus the measurement time.

However, after three 5-minute heating increments, a new phenomenon was realized. After equilibration to room temperature, the first measurements taken with DLS showed spikes in intensity. Intensity spikes are indicative of large particles diffusing into and out of the laser light. Because the solutions are sealed, these large particles must be formations of insulin aggregates. However, these spikes were not repeated in subsequent measurements. Figure 6 shows two of the measurements taken after three 5-minute heating periods.

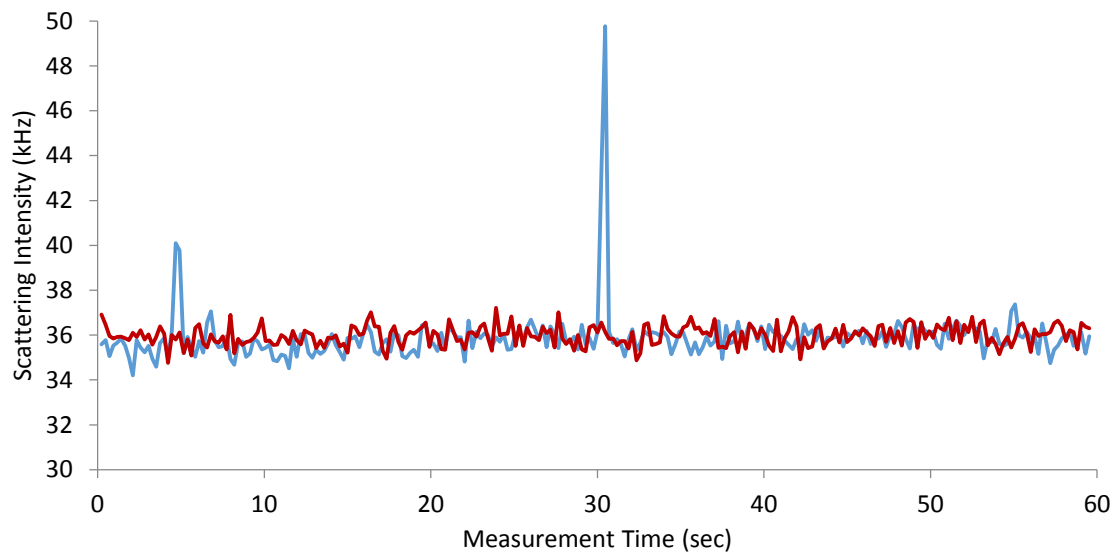


Figure 6: Insulin scattering intensity measurements taken after three 5-minute heating increments, totaling 15 minutes at heat. The blue line is first measurement taken after equilibration to room temperature.

The phenomenon witnessed in Figure 5 was repeated after heating for an additional 5-minute increment. The total time spent on heat is now 20 minutes. After equilibration to room

temperature, even more intensity spikes were present. Again, these spikes decay into a relatively flat intensity baseline. Figure 7 shows the measurements taken after four 5-minute heating periods.

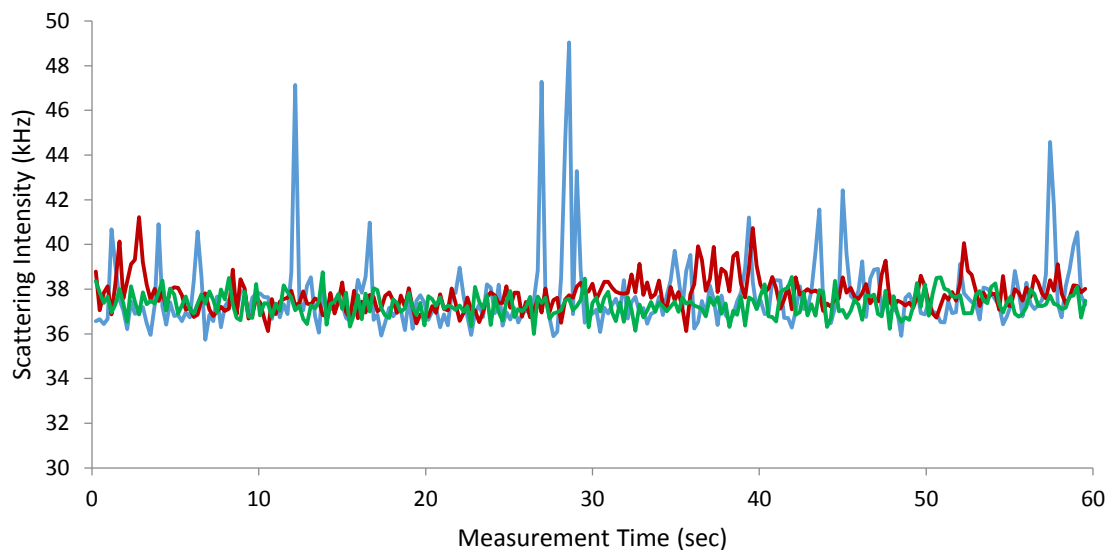


Figure 7: Insulin scattering intensity measurements taken after four 5-minute heating increments, totaling 20 minutes at heat. The blue line is first measurement taken after equilibration to room temperature; red, the second, and green, later.

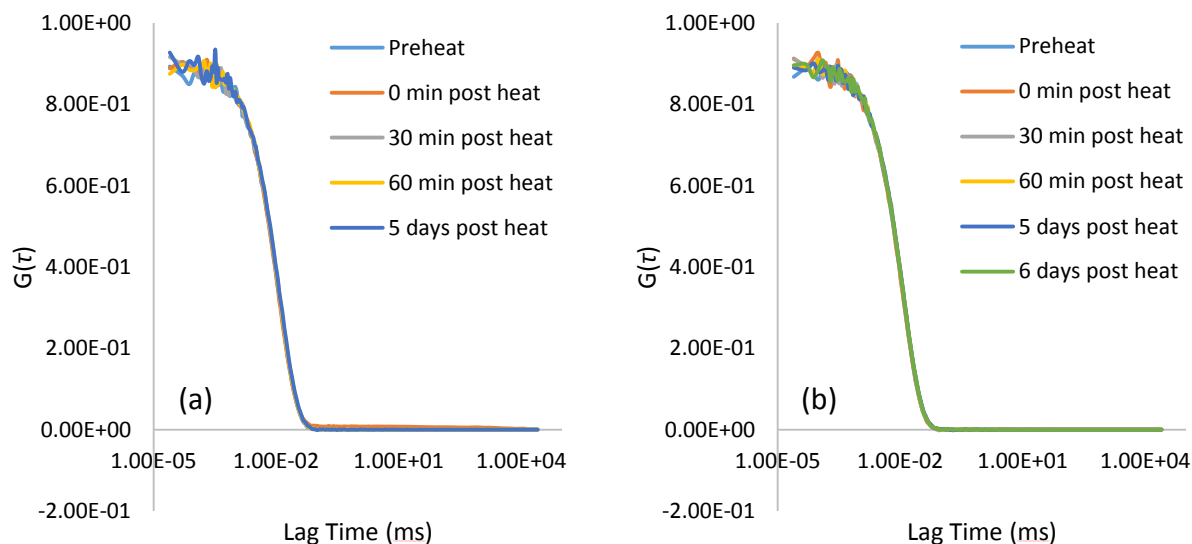
The presence of intensity spikes is indicative of large particles forming in solution after heating. These aggregates dissociate after time spent at room temperature. However, it is important to note that the intensity baseline that is realized in Figures 6 and 7 is not equal to the initial intensity baseline of 35 kHz; it is slightly higher (around 38 kHz after 20 minutes at heat). Although the large particles that cause the intensity spikes are disappearing, some permanent aggregation is present.

Study results

The preliminary study showed that the larger aggregates formed after heating will dissociate after thermal quenching to room temperature. The study described in the *Sample Heating* section above aims to assess the nature of these supposedly permanent aggregates and

assess the reversibility of aggregation induced with shorter heating times. Based on the aforementioned preliminary results, identical solutions of insulin were heated for 10, 15, 25, and 29 minutes in order to assess even earlier stages in the aggregation process. The autocorrelation functions, hydrodynamic radius peak distributions and widths, and scattering intensity measurements for those samples are discussed below.

The autocorrelation functions for the heated samples are shown below in Figure 8. They show the average autocorrelation functions generated at specified times after the samples are removed from heat. The autocorrelation function, as discussed earlier, represents the decay in signal as lag time grows. If two distinct particle size populations were present at the time of a single measurement, the functions would show two decays. If population size was relatively uniform but changing over time, for instance during the time after heating, the functions would decay more slowly, reaching zero at larger and larger lag times.



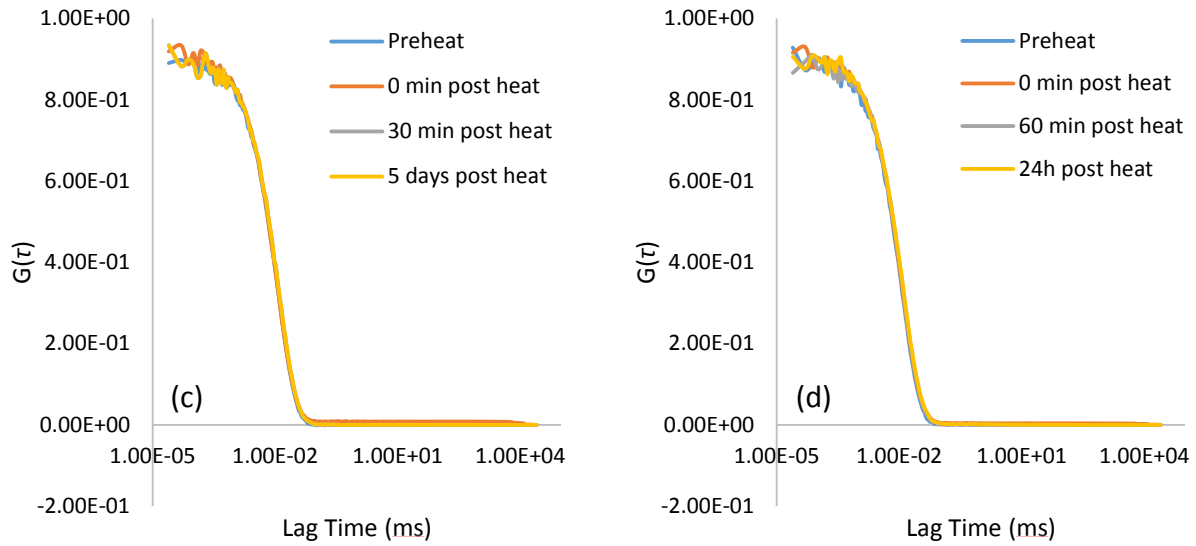
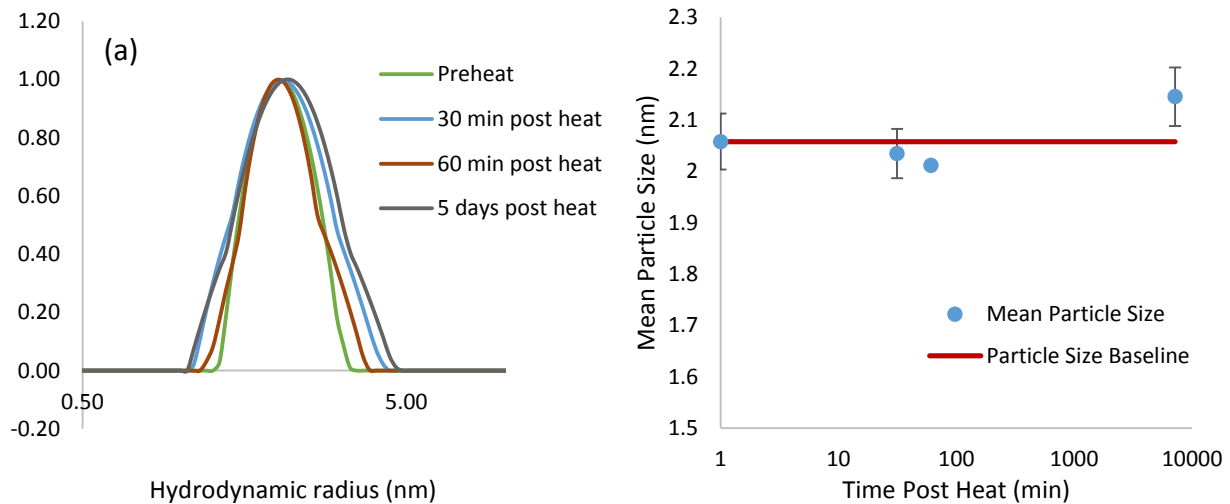


Figure 8: Autocorrelation functions at various times after removal from heat for samples heated (a) 10, (b) 15, (c) 25, and (d) 29 minutes, respectively.

As shown, the functions show near-identical decays, with the exception of some of the measurements taken immediately after removal from heat, likely an artifact of temperature gradient between the warm solution and room temperature instrument. This result lends one to conclude that not much aggregates during the studied period. This is confirmed by the derived particle size distributions, calculated as described previously. Figure 9 shows the averaged size distributions and mean particle sizes as a function of time after removal from heat.



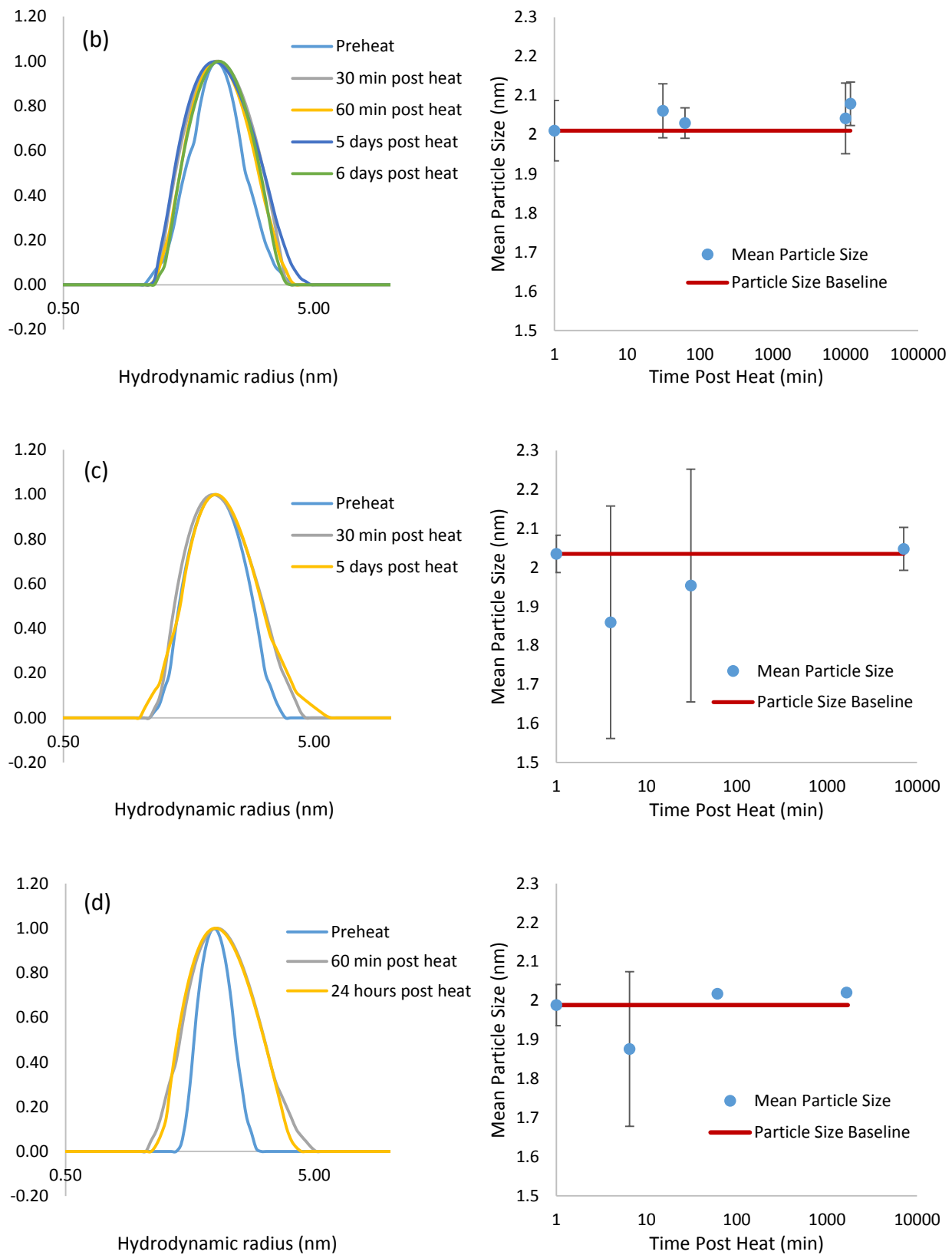


Figure 9: Hydrodynamic radii peak distributions and mean particle sizes for samples heated (a) 10, (b) 15, (c) 25, and (d) 29 minutes, respectively.

The figures above show very little statistical difference in the time after heating, regardless of heat time, indicating that the majority of the population is still in monomeric form. However, the peak distributions are much clearly different after heating for all trials. The peaks exhibit broadening as a small fraction of the population becomes slightly larger, enough to skew the peak without generating a new distribution. This is thought to be the formation of dimers from monomers. The widths of the peaks are quantified and plotted below in Figure 10.

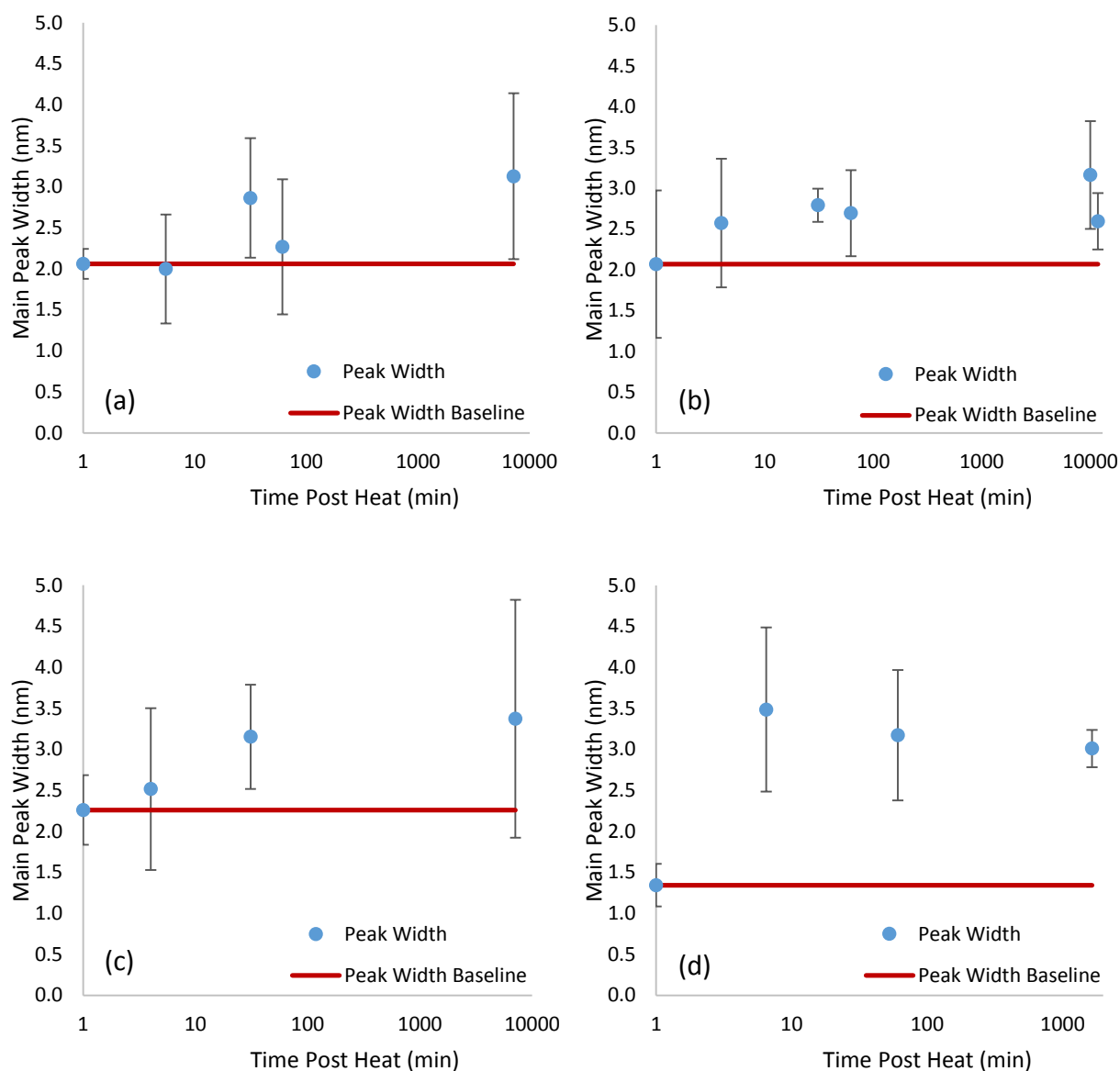


Figure 10: Calculated hydrodynamic radius peak distribution widths versus time after removal from heat for samples heated (a) 10, (b) 15, (c) 25, and (d) 29 minutes, respectively

The high standard deviations in Figure 6 are likely due to the fact that at any given time, particles are diffusing into and out of the laser light. The averages taken in order to form the above plots group measurements of 60 seconds across times as different as 8-10 minutes, meaning it is likely that many different particles are present for each measurement. Given the small amount of particles that are actually aggregating, this can have a substantial effect on the hydrodynamic radius calculation.

The samples heated for 10 minutes show an average peak broadening that is not statistically significant. Samples heated for 15 minutes show a similar trend with slightly more statistical significance, and samples heated for 25 and 29 minutes show statistically significant broadening. Because the absolute peak width values can vary between samples, it is best to compare their changes after heating. Figure 11 shows the relative broadening after the samples were removed from heat.

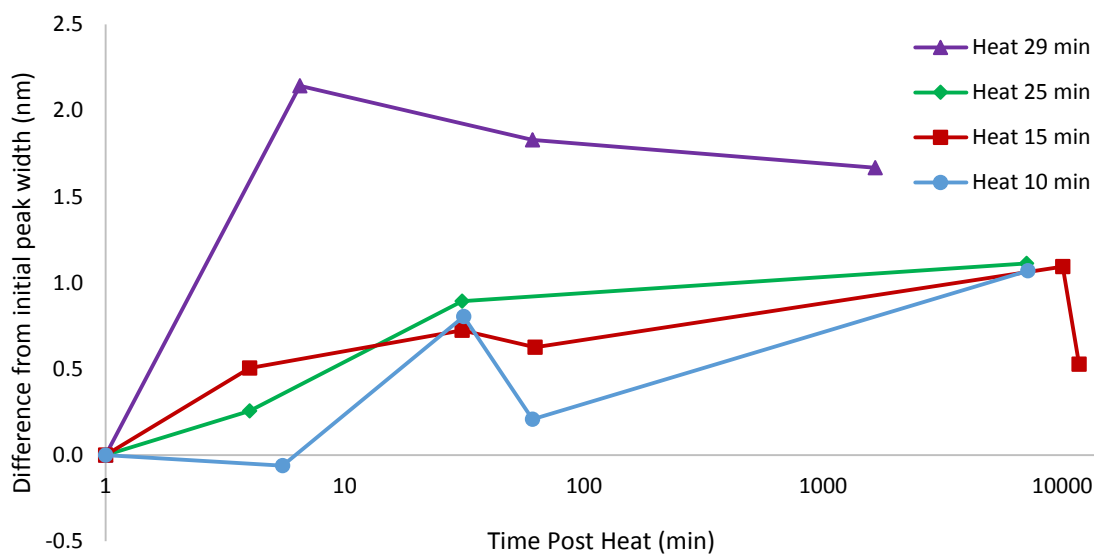


Figure 11: Peak broadening versus time after removal from heat for all samples

In all samples, the broadening does not significantly decrease at any point after removal from heat. This indicates that the formed dimers do not return to monomers by thermal quenching. This conclusion is supported by not only the peak distribution data in Figure 8 but

also by the scattering intensity measurements from each sample. As previously mentioned, the scattering intensity is proportional to the size of the dissolved particles when concentration is kept constant. This assumption is valid for this system because since only a small amount of the particles are aggregating, the concentration can be assumed unchanged. The intensity measurements for the samples are shown below in Figure 12.

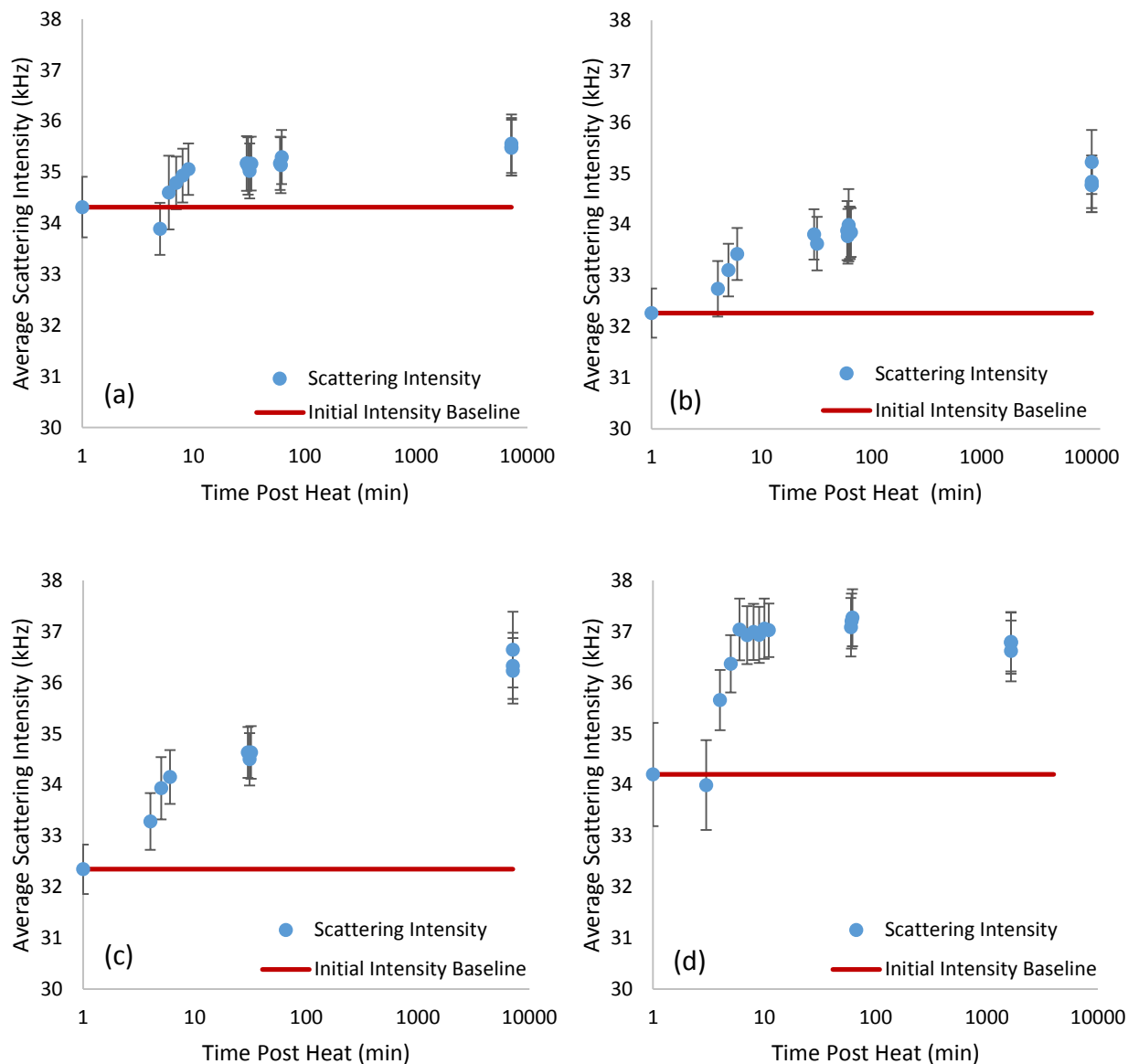


Figure 12: Scattering intensity data versus time after removal from heat for samples heated (a) 10, (b) 15, (c) 25, and (d) 29 minutes, respectively

Like the peak width, in order to compare the samples it is best to look at the relative change in intensity versus time due to the variable nature of the absolute measurement. Figure 13 shows the increase in intensity from the initial preheat baseline plotted against time after removal from heat.

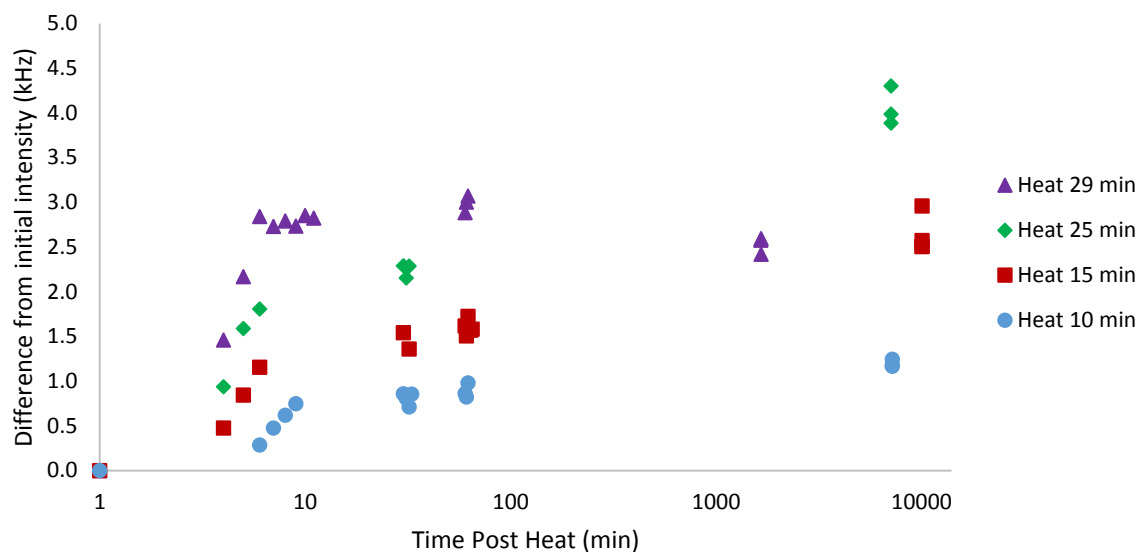


Figure 13: Intensity increase from preheat baseline versus time after removal from heat.

Like the peak width, the intensity does not decrease over time after removal from heat, indicating that the cause of the intensity increase is still present. As previously mentioned, it is thought that the increase is caused by a small amount of dimer in solution. As expected, the samples display an intensity increase relative to the time spent on heat, i.e. the sample that was heated the longest displays the largest intensity gain, etc.

Conclusions and Future Work

From the experiments performed in this study, it is clear that even just 10 minutes of heating produces aggregation that is irreversible by thermal quenching. The aggregation is most likely from monomer to dimer and only for a tiny portion of the particles in solution. Due to the nature of this aggregation, it is apparent that the studied realm is still in the slow initial realm of the sigmoidal aggregation curve. This is in contrast with the formation of larger aggregates that produce significant spikes in scattering intensity, which disappear after thermal quenching to room temperature. Proposed mechanisms of insulin aggregation suggest a slow and potentially reversible nucleation step. The initial step in the heat induced aggregation of insulin is shown to be different.

There is much potential for the continuation of this project. Of course, similar studies can be performed on insulin samples heated for shorter times; for instance 2, 5, 7, and 10 minutes. Because this heat times in this study were too long, despite the small amount of aggregation attained, shorter heat times will yield different and potentially more favorable reversibility results. However, according to the results of this study, it is likely that once any dimerization occurs, the formed aggregate is permanent, despite the shorter length of heating.

Additionally, the University of Connecticut Institute of Materials Science recently purchased a Bruker Small Angle X-Ray Scattering (SAXS) instrument. SAXS added capabilities over DLS, including the ability to distinguish morphology. Where DLS does not take into account shape when determining hydrodynamic radius, SAXS can actually produce information about particle shapes. This is particularly valuable for this study because the morphology of the insulin is changing as it aggregates. This analysis could yield critical information about the specific mechanisms of amyloid aggregation and potential for reversibility.

References

- (1) “Alzheimer’s Disease Fact Sheet.” Alzheimer’s Disease Education & Referral Center. National Institute of Health, 11-6423. July, 2011.
- (2) “The role of Plaques and Tangles.” The Alzheimer’s Association.
<http://www.alz.org/alzheimers_disease_what_is_alzheimers.asp#tangles> (accessed Jan 27, 2013).
- (3) Murphy, S. L., Xu, J., Kochanek, K. D. “Deaths: Final Data for 2010.” National Vital Statistics Reports, v61, 4. May 8, 2013.
- (4) “Medications for Memory Loss.” The Alzheimer’s Association.
<http://www.alz.org/alzheimers_disease_standard_prescriptions.asp> (accessed Mar 6, 2014).
- (5) Pease, L., Sorci, M., Guha, S., Tsai, D., Zachariah, M., Tarlov, M., Belfort, G. 2010. Probing the Nucleus Model for Oligomer Formation during Insulin Amyloid Fibrillogenesis. *Biophysical Journal*, 99, 3979-3985.
- (6) Murphy, R. M. 2007. Kinetics of amyloid formation and membrane interaction with amyloidogenic proteins. *Biochimica et Biophysica Acta* 1768, 1923-1934.
- (7) “The Hallmarks of AD.: The National Institute on Aging, National Institute of Health.
<<http://www.nia.nih.gov/alzheimers/publication/part-2-what-happens-brain-ad/hallmarks-ad>> (accessed Mar 3, 2014).
- (8) Shankar, G. M., S. M. Li, ... , D. J. Selkoe. 2008. Amyloid-b protein dimers isolated directly from Alzheimer’s brains impair synaptic plasticity and memory. *Nature Medicine* **14**, 837–842.
- (9) Brange, J., Anderson, L., Laursen, E., Meyn, G., Rasmussen, E. 1997. Toward Understanding Insulin Fibrillation. *Journal of Pharmaceutical Sciences*, 86, 5, 517-525.

- (10) Hua, Q., Weiss, M. 2004. Mechanism of Insulin Fibrillation. *Journal of Biological Chemistry*, 279, 20, 21449-21460.
- (11) Ahmad, A., Uversky, V. N., Hong, D., Fink, A. “Early Events in the Fibrillation of Monomeric Insulin.” *Journal of Biological Chemistry*, v280, 52. 42669-42675. 2005.
- (12) Jansen, R., Dzwolak, W., Winter, R. “Amloidogenic Self-Assembly of Insulin Aggregates Probed by High Resolution Atomic Force Microscopy.” *Biophysical Journal*, v88. 1344-1353. 2005.
- (13) ALV/CGS-3 MD Preview. ALV.
<http://www.alvgmbh.de/Products/goniometers/ALV_CGS3MD/alv_cgs3md.html>
(Accessed Mar 3, 2014).
- (14) Liu, Y., Li, M., Yang, Y., Xia, Y., Nieh, M. -P. “The Effects of Temperature, Salinity, Concentration and PEGylated Lipid on the Spontaneous Nanostructures of Bicellar Mixtures.” In Press, 2014.
- (15) Berne, B. J., Pecora, R. “Dynamic Light Scattering With Applications to Chemistry, Biology, and Physics.” Toronto, Ontario. General Publishing Company, Ltd. 2000.
- (16) Nieh, M. -P., Harroun, T. A., Raghunathan, V. A., Glinka, C. J., Katsaras, J.
“Spontaneously Formed Monodisperse Biomimetic Unilamellar Vesicles: The Effect of Charge, Dilution, and Time.” *Biophysical Journal*, 86. 2615-2629. April 2004.